BAMS Article

Fire and Rain

The Legacy of Hurricane Lane in Hawai'i

Alison D. Nugent, Ryan J. Longman, Clay Trauernicht,
Matthew P. Lucas, Henry F. Diaz, and Thomas W. Giambelluca

ABSTRACT: Hurricane Lane (2018) was an impactful event for the Hawaiian Islands and provided a textbook example of the compounding hazards that can be produced from a single storm. Over a 4-day period, the island of Hawai'i received an island-wide average of 424 mm (17 in.) of rainfall, with a 4-day single-station maximum of 1,444 mm (57 in.), making Hurricane Lane the wettest tropical cyclone ever recorded in Hawai'i (based on all available quantitative records). Simultaneously, fires on the islands of nearby Maui and O'ahu burned 1,043 ha (2,577 ac) and 162 ha (400 ac), respectively. Land-use characteristics and antecedent moisture conditions exacerbated fire hazard, and both fire and rain severity were influenced by the storm environment and local topographical features. Broadscale subsidence around the storm periphery and downslope winds resulted in dry and windy conditions conducive to fire, while in a different region of the same storm, preexisting convection, incredibly moist atmospheric conditions, and upslope flow brought intense, long-duration rainfall. The simultaneous occurrence of rain-driven flooding and landslides, high-intensity winds, and multiple fires complicated emergency response. The compounding nature of the hazards produced during the Hurricane Lane event highlights the need to improve anticipation of complex feedback mechanisms among climate- and weather-related phenomena.

https://doi.org/10.1175/BAMS-D-19-0104.1
Corresponding author: Alison D. Nugent, anugent@hawaii.edu
In final form 27 January 2020

AFFILIATIONS: Nugent—Department of Atmospheric Sciences, University of Hawai'i at Mānoa, Honolulu, Hawai'i; **Longman**—East West Center, Honolulu, Hawai'i; **Trauernicht**—Department of Natural Resources and Environmental Management, University of Hawai'i at Mānoa, Honolulu, Hawai'i; **Lucas and Diaz**—Department of Geography and Environment, University of Hawai'i at Mānoa, Honolulu, Hawai'i; **Giambelluca**—Water Resources Research Center and Department of Geography and Environment, University of Hawai'i at Mānoa, Honolulu, Hawai'i

Severe tropical cyclones are arguably the most destructive storms on Earth. Commonly referred to as "hurricanes" in the North Atlantic and eastern North Pacific, "typhoons" in the western North Pacific, and "cyclones" elsewhere, these storms pose multiple threats to the people and property that lie in their paths. Research on fatalities from Atlantic tropical cyclones has shown that the most lethal aspects of these storms are (beginning from the most severe threat) storm surge, rain, wind, and coastal and offshore hazards such as waves and rip currents (Rappaport 2014). Although the specific threats vary from storm to storm and place to place, single storm events pose multifaceted and potentially cumulative hazards.

The vulnerability of a population in any given location to the impacts of tropical cyclone hazards is determined by and mediated by a multitude of interacting factors. Biophysical aspects include distance inland from the coast, terrain slope, coastal ecosystem integrity, and land surface cover. Socioeconomic factors include infrastructure quality, the availability of early warning systems, and capacity for evacuation and emergency response. The combination of biophysical and socioeconomic factors influences the severity of storm impacts in any given place (Turner et al. 1996).

In Hawai'i, landfall by hurricanes is relatively rare due to persistent vertical wind shear over the islands. The earliest report of a major hurricane causing severe damage in Hawai'i dates back to 1871 (Businger et al. 2018) and since 1950, only five hurricanes (Nina in 1957, Dot in 1959, Iwa in 1982, Estelle in 1986, and Iniki in 1992) have caused serious damage to the main islands of Hawai'i (Smith et al. 2012). Hurricane Iniki (1992) was the strongest and most destructive of these storms, with sustained 145-mph (1 mph $\approx$ 0.45 m s^{-1}) winds just prior to landfall, that caused an estimated US$1.8 billion in property damage and six fatalities (Brown et al. 1993). When hurricanes do occur near Hawai'i, the geography of the islands can exacerbate the hazards. The nearly 1,200 km (746 mi) of coastline makes much of the state susceptible to coastal flooding, and the mountainous topography can enhance atmospheric lifting and subsequent high-intensity rainfall, as well as intensifying wind speeds. In addition, the steep mountainous terrain can enhance flash flooding and trigger landslide events.

The 2018 Northern Hemisphere hurricane season was especially active, with a combined total of 66 storms occurring in the Atlantic and Pacific basins. The Atlantic basin had 15 named storms, including 8 hurricanes and 2 major hurricanes (>111-mph sustained winds, equivalent to category 3, 4, or 5 on the Saffir–Simpson scale; NOAA/NHC 2019), while the central and eastern Pacific had 22 total named storms, including 13 hurricanes and 10 major hurricanes (NOAA/CPHC 2019). Activity from these storms set a new record for accumulated cyclone energy, a measure of total wind energy, in the northeast Pacific since 1971 when the record began (Klotzbach and Bell 2018). Anomalously warm sea surface temperatures (SSTs) were found across the world (NOAA/NCEI 2019), and the global ocean surface heat content (upper 700 m) for July–September 2018 was the highest since records began in 1955 for both the Atlantic and Pacific basins (NOAA/NCEI 2018). Increased ocean heat is potentially explained by El Niño–Southern Oscillation, which developed from a neutral phase over the summer of 2018 leading to El Niño (warm) conditions that emerged in September and persisted through the following winter.

Around the Hawaiian Islands, SSTs were just above 27°C throughout August 2018, slightly higher than the 26.7°C seasonal average in the region (Coral Reef Watch 2019), and over a 2-month period (8 August–4 October) five hurricanes tracked within 445 km (275 mi) of the island

chain. Hurricanes Hector (category 4), Lane (category 5), Norman (category 4), Olivia (category 4), and Walaka (category 5) all entered Hawaiian waters, causing varying degrees of damage in the islands. Of these storms, only Olivia made landfall on the main Hawaiian Islands, after being downgraded to a tropical storm. Hurricane Walaka (ranked the second strongest tropical cyclone ever recorded in the central Pacific) passed near to and essentially destroyed East Island, one of the unpopulated northwestern Hawaiian Islands (NOAA/CPHC 2018). Hurricane Lane (hereafter, Lane) was by far the costliest storm of the 2018 hurricane season in Hawai'i. Despite never making landfall, Lane caused considerable damage and disruptions across the state, including severe flooding on the island of Hawai'i and multiple fires on the islands of Maui and O'ahu. In fact, the damages from the floods and fires were so severe that it prompted the U.S. government to issue a major disaster declaration for this event (FEMA 2018).

Hurricane–fire interactions have been documented in the literature (Myers and van Lear 1998; Liu et al. 2008; Platt et al. 2002; Christopher et al. 2009). The general hypothesis is that fire hazard can increase after an intense hurricane due to greater fuel loads from downed woody debris and litter, and lower fuel moistures due to increased insolation and higher wind speed under an open canopy (Myers and van Lear 1998). Liu et al. (2008) showed that on the Gulf of Mexico coast, the highest-intensity fires tended to occur within years or decades after a catastrophic hurricane strike. However, real-time interactions of hurricane and concurrent fire events are very rarely reported. The only two we have found documented are Subtropical Storm Andrea (2007), which exacerbated fires already burning in the Okefenokee National Wildlife Refuge across Florida and Georgia (Christopher et al. 2009; Barbero et al. 2015; FDEM 2011), and a recently reported connection between storm-force winds from Hurricane Ophelia (2017) and wildfires in Portugal (Fernandes 2018). While heavy rain is a familiar feature of tropical storms, the strong convection near the storm center is also associated with, or perhaps compensated by, descending air around the storm's periphery (Fett 1964). This subsiding air is warm and dry, and together with intense storm-driven winds, we hypothesize this could increase the risk of fire hazard in the periphery of the hurricane, especially if preexisting conditions predisposed the area to fire. The potential for compounding hazards warrants further exploration, and to date, the authors are not aware of any work documenting the simultaneous occurrence of both heavy rainfall and fire during a hurricane event. The Lane event therefore provides a compelling case study of how atmospheric conditions associated with hurricanes can simultaneously contribute to record rainfall and increased fire risk.

The primary objective of this study is to present a detailed analysis of the multiple hazards associated with the passage of Lane in the Hawaiian region over the 4-day period of 22–25 August 2018 (Fig. 1) and to determine how simultaneous fire and rain impacts from a hurricane can both be possible. First, we provide a synopsis of the storm. Next, we draw on several data sources to identify and characterize how environmental conditions contributed to intense rainfall and severe flooding on the island of Hawai'i and to multiple wildfires that occurred on the islands of Maui and O'ahu during the storm passage. Finally, we discuss land use changes that are likely to impact fire risk, terrain interactions that can exacerbate hazards associated with wind and rain, and specific features of the hurricane environment.

Datasets and methods

A combination of surface observations were used to investigate the storm environment with a focus on precipitation and fire weather.

Rainfall data. Daily precipitation data were used to characterize the Lane event and the months leading up to it. These data were obtained from several national online data repositories including the National Center for Environmental Information (NCEI; www.ncei.noaa.gov/) and the Hydrometeorological Automated Data System (HADS; https://hads.ncep.noaa.gov/) along with

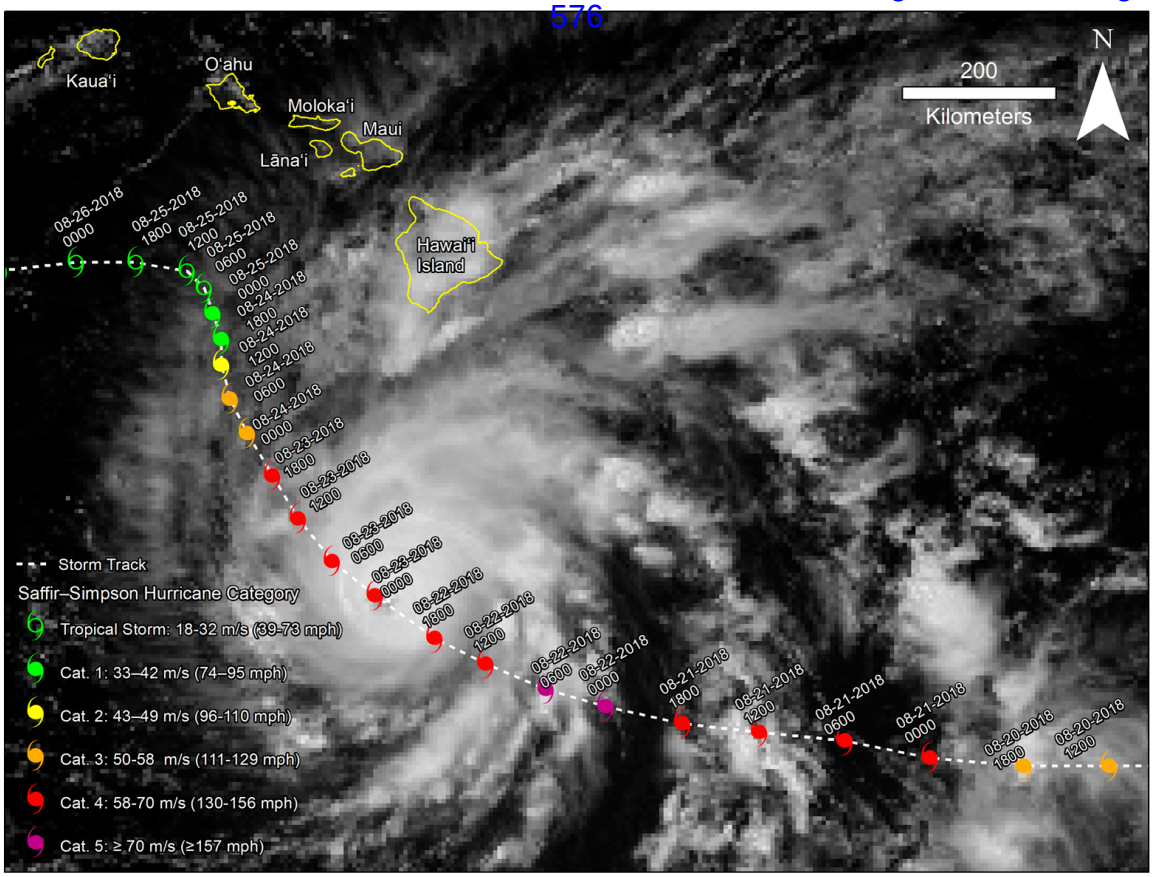

Fig. 1. The background image shows a visible image from *GOES-15* of Hurricane Lane at 2300 UTC 22 Aug 2018 when its eye was centered at ~15°31′00″N, 156°11′00″W near the Hawaiian Islands in the central Pacific . The white dashed line indicates the best track of Lane (Knapp et al. 2010), labeled with dates and times (UTC), and the color of the hurricane symbol indicates the strength of winds in the storm.

additional data from various local networks. A 25-yr (1990–2014) time series of daily rainfall maps on a 250-m grid were utilized to characterize past rainfall events [see Longman et al. (2018) for a complete description of local networks and data sources in Hawai'i]. In total, 156 rainfall stations with continuous data over the 4-day event were identified across the state (Fig. 2). Mean monthly rainfall climatologies were obtained from the Rainfall Atlas of Hawai'i (Giambelluca et al. 2013).

Meteorological stations. The atmospheric conditions contemporaneous with wildfires on Maui and O'ahu during the Lane event are examined using hourly and daily observations of "fire weather" variables based on the National Weather Service (NWS) red flag warning criteria for Hawai'i (NWS/HFO 2018a). The NWS tracks the daily Keetch–Byram drought index (KBDI), hourly wind speed, and relative humidity (RH) at the Daniel K. Inouye International Airport (PHNL) in Honolulu and uses the thresholds indicated in Fig. 3 to declare red flag warnings for high fire danger when all thresholds are crossed and maintained for at least 2 h. KBDI is calculated from mean annual rainfall, daily rainfall, and temperature, such that the KBDI value indicates the quantity of rain (mm) necessary to saturate the soil. Larger KBDI values indicate more severe drought conditions, and over time the value of KBDI steadily increases when no rain is received. As a daily index, KBDI captures short-term fluctuations in moisture availability and performs well for fire prediction in tropical and subtropical climates such as Hawai'i (Dolling et al. 2005; Brolley et al. 2007). In Fig. 3, KBDI was derived from NWS calculations at PHNL; however, RH and wind data were obtained from Kapalua Airport (PHJH) in Lahaina, Maui, and

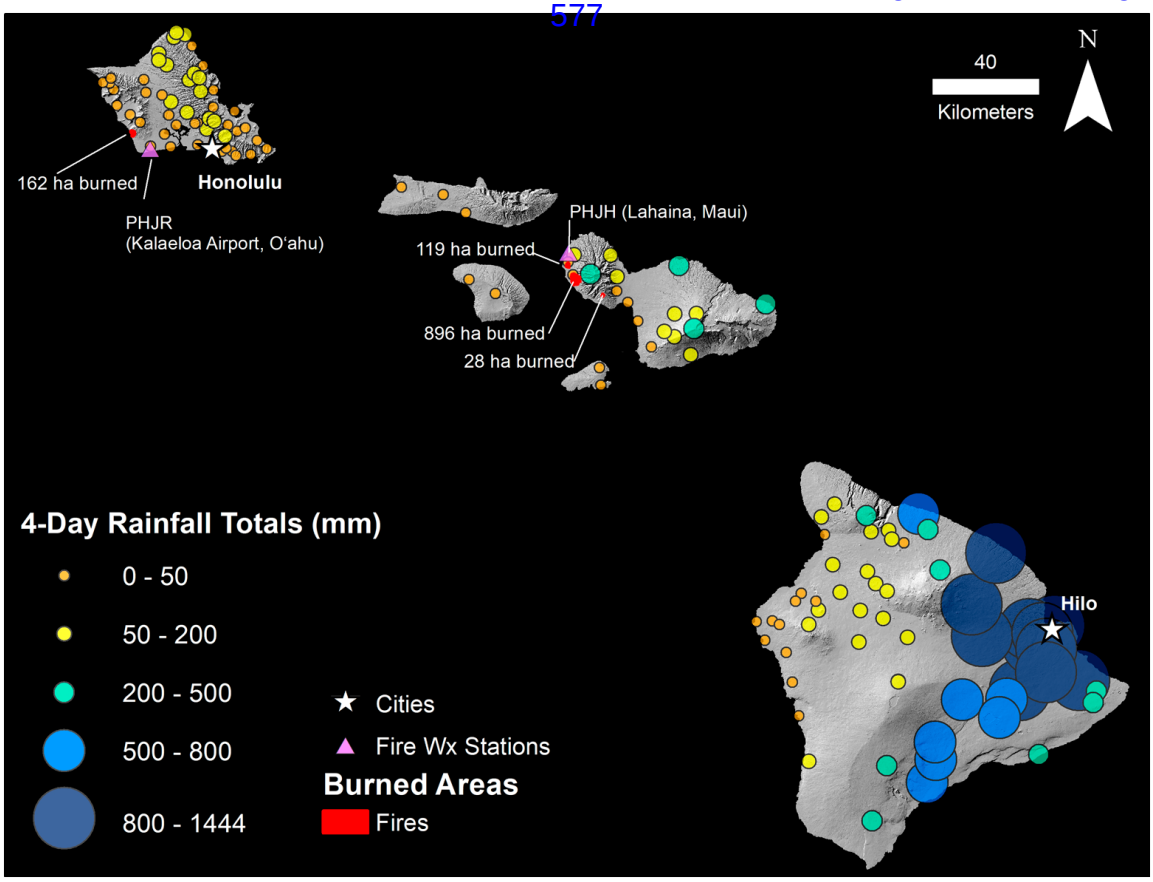

Fig. 2. Map highlighting the locations impacted by heavy rainfall and fire in the Hawaiian Islands. Circular dots indicate the location of rain gauges used for estimating precipitation from Hurricane Lane, and the 4-day accumulated rainfall totals (mm) from 22 to 25 August 2018. Also included are the locations of the wildfires on Maui and O'ahu, with their burned areas denoted in red, and the locations of the Kalaeloa Airport (PHJR) and Lahaina, Maui (PHJH), weather stations used for analysis denoted with purple triangles.

Kalaeloa Airport (PHJR) on O'ahu, the closest high-quality weather stations to the fires. Drought status was also characterized using the National Drought Monitor (Svoboda et al. 2002) conditions at the fire locations. Finally, the Hilo radiosonde sounding (PHTO) was utilized for time series of the vertical profile of atmospheric conditions.

Fire extent and land cover. The areas burned by fires on Maui and O'ahu were mapped in Google Earth Engine using *Sentinel-2* satellite images captured within 2 months following the fires (Drusch et al. 2012). Land cover on the islands and within the burned areas was obtained from a 2.4-m resolution NOAA Coastal Change Analysis Program (C-CAP) land cover product (Klemas et al. 1993), last updated for Maui in 2010 and for O'ahu in 2011.

Rainfall mapping. Following methods similar to those used by Longman et al. (2019), daily precipitation maps were created for the island of Hawai'i using an inverse distance weighting (IDW) approach combined with climatologically aided interpolation (Willmott and Robeson 1995). For each day, anomalies were calculated as the ratio of station daily rainfall to mean daily rainfall retrieved from the Rainfall Atlas of Hawai'i at the station location (Giambelluca et al. 2013). Station anomalies were then interpolated to a 250-m grid for each island. Finally, the gridded daily anomalies were multiplied by the gridded daily mean to produce a daily rainfall map. The 4-day Lane event rainfall was calculated as the sum of the four-daily (midnight to midnight local time) rainfall grids within 22–25 August 2018 time period. Finally,

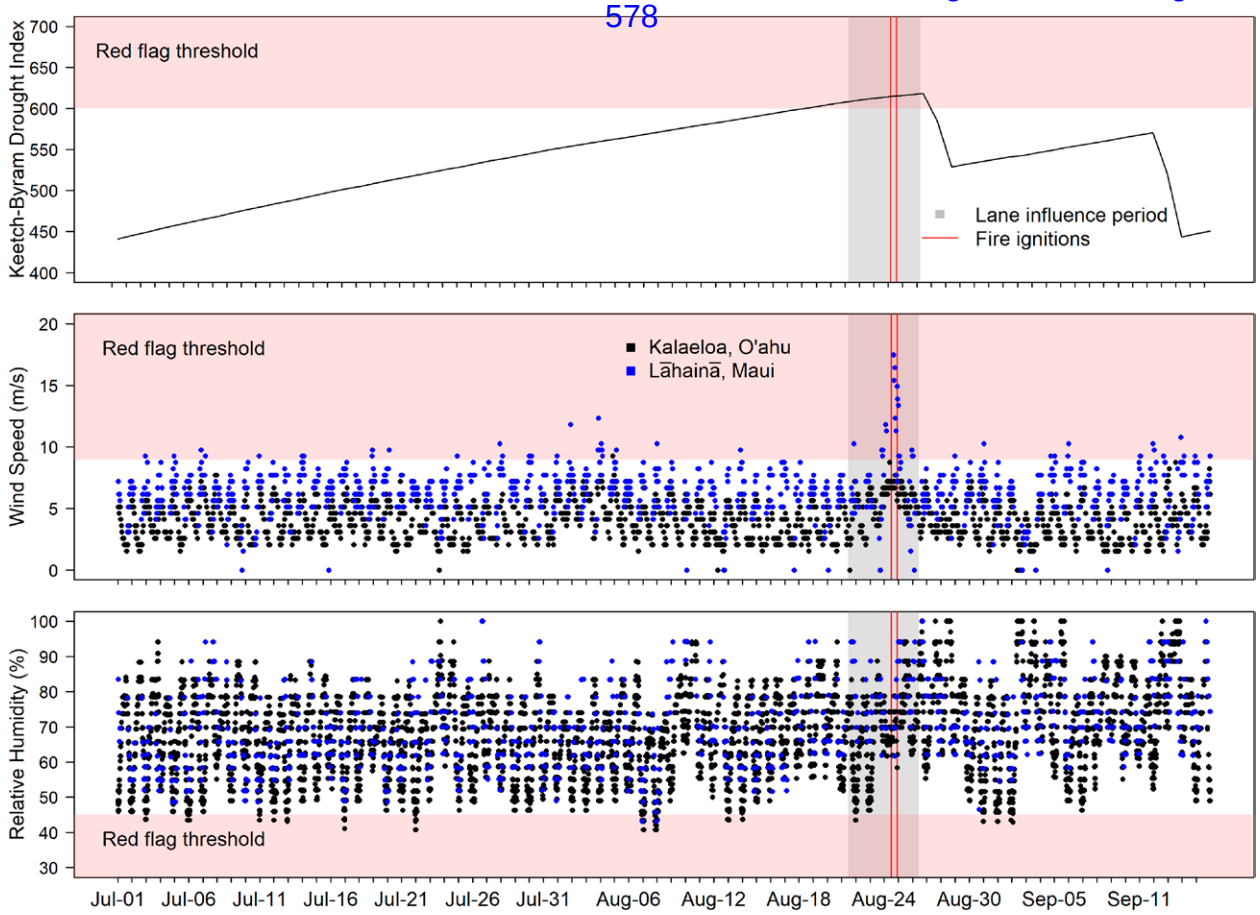

Fig. 3. Time series of fire weather variables for the time well before, during, and after Lane from 1 Jul to 15 Sep 2018 HST showing the red flag warning variables and thresholds for wildland fire danger used by the NWS Honolulu Forecast Office (HFO). (top) Daily KBDI, as calculated by the NWS, is shown for the Honolulu Airport. Hourly (middle) wind speed (m s^{-1}) and (bottom) RH (%) are shown for the two NWS stations closest to the active forest fires on Maui (Lahaina, Maui; PHJH) and O'ahu (Kalaeloa Airport; PHJR). Also shown are the ignition times (vertical red lines) indicating the start times of the west Maui fires during the early morning on 24 Aug 2018 (Kau'aula and Kā'anapali fires) and the west O'ahu Kahe Point Power Plant fire at midday on 24 Aug 2018.

4-day Lane rainfall was compared to rainfall for all 4-day periods in the 25-yr daily gridded rainfall time series.

Our methods of rainfall mapping during the Lane event differ from those of Longman et al. (2019) in that we use all available stations (as opposed to the closest five) in the interpolation of anomalies and a weighting parameter of 1 (as opposed to 1.5). These parameters were updated as a result of optimization conducted during this present analysis and are specific to the island of Hawai'i. To enable comparison between Lane and past events, we reanalyzed the entire 25-yr (1990–2014) set of daily rainfall maps from Longman et al. (2019) using this new optimization scheme.

Results

Hurricane Lane synopsis. According to the National Hurricane Center (NHC) tropical cyclone report (Beven and Wroe 2019), Lane was declared a tropical depression at 0000 UTC 15 August, intensified into a tropical storm 12 h later, and reached hurricane status at 0000 UTC 17 August. Rapid intensification during the next 30 h elevated the storm to category 4 strength by 0600 UTC 18 August. As Lane crossed into the central Pacific basin (nominally, west of 140°W), it was weakened by vertical wind shear and downgraded to a category 3 storm. Soon after, Lane reintensified back into a category 4 hurricane on 20 August, eventually reaching category

5 intensity just after 1800 UTC 21 August (as determined by NOAA aircraft; Beven and Wroe 2019). Lane peaked with 160-mph winds and a central pressure of 926 hPa on 22 August, while located approximately 320 miles (515 km) south-southeast of the island of Hawai'i. As Lane approached the Hawaiian Islands, it began to weaken as vertical wind shear intensified once again, and was downgraded to a tropical storm at 0600 UTC 25 August. The initial westward track of Lane was controlled by the semipermanent high pressure system located to the northeast of the Hawaiian Island chain. As the high pressure system weakened (on 23 August), Lane made a near 90° turn north and in multiple forecasts from 20 to 23 August, the cone of uncertainty allowed for landfall on O'ahu and Maui at hurricane strength. Instead, the storm was weakened as a result of vertical wind shear, thus allowing the lower level trade winds to advect it westward, prompting a second 90° turn in the storm track and removing the threat of landfall on any of the main Hawaiian Islands. Lane's initial path, strength, and late August timing were reminiscent of Hurricane Dot (1959). The primary differences between the two storms being that Dot continued to move Northward while Lane was advected westward before landfall and Lane produced significantly more rainfall than Dot for the Hawaiian Islands.

As Hurricane Lane approached the island chain, the island of Hawai'i was located in the right-front quadrant of the storm, a favorable area for enhanced convective activity and precipitation in hurricanes (Corbosiero and Molinari 2003; Lonfat et al. 2004). Although the center of Lane did not pass closer than 140 miles (225 km) from the island of Hawai'i, its large circulation and slow translation speed brought prolonged torrential rains which resulted in flooding, mudslides, and landslides across many parts of the island of Hawai'i and various other parts of the state.

Environmental evolution. Meteorological time series are shown for fire weather variables from 1 July to 15 September 2018 at Kalaeloa Airport, O'ahu, and Lahaina, Maui, in Fig. 3. The closest approach of Lane (131 mi or 212 km) from Honolulu occurred at 1200 UTC (0200 HST) 25 August. The fire weather variables indicate that preexisting drought and high winds due to Lane were key factors driving fire occurrence and spread. KBDI values crossed and remained above the Red Flag threshold of 600, suggesting increased risk of fire danger from 18 to 26 August at the wildfire locales. Furthermore, the U.S. Drought Monitor for the same time period indicated "abnormally dry" to "moderate drought" conditions at those same locations. The most anomalous weather condition during the Lane influence period was the elevated surface wind speeds recorded at both the Lahaina and Kalaeloa station on 24 August, coinciding with the initiation of the O'ahu and Maui fires. Winds at Lahaina clearly exceeded the red flag threshold (8.9 m s^{-1} or 20 mph for >2 h), while winds at Kalaeloa, though elevated, did not cross the Red Flag threshold. This is perhaps due to the station position south of, rather than downwind of the Wai'anae mountain range. Minimum RH reached near or below the Red Flag threshold (45%) at Kalaeloa on 21 August (43%) and 22 August (46%) as Lane approached, but was above the threshold at both stations at the time of the fires.

Shifts in atmospheric conditions were also observed throughout the atmospheric column preceding and during the passage of Lane (Fig. 4) from vertical atmospheric profile data retrieved from the Hilo sounding for the period 16–31 August 2018. As Lane approached (21–22 August), temperatures were slightly elevated at all significant levels and vapor pressures were slightly depressed. This observed warming and drying was followed by a steep rise in vapor pressure (beginning on 22 August) especially in the midlevels, along with maxima in wind speeds occurring throughout the vertical profile (23–24 August).

Wildfires. Beginning on 24 August, three wildfires were detected on Maui and one on O'ahu, all of which occurred on the drier, leeward slopes of both islands. The incidents on Maui included (i) a 28-ha fire at Mā'alaea ignited at 2300 HST 23 August, self-extinguished due to heavy rainfall generated by the storm that was not included in our analysis; (ii) a 896-ha fire near

Lahaina (the "Kaua'ula Fire") that ignited at 0100 HST 24 August; and (iii) a 119-ha fire at Kā'anapali that ignited at 0730 HST 24 August. On O'ahu, a 162-ha fire ignited near the Kahe Point Power Plant around 1100 HST 24 August. Nonnative, fire-prone grass- and shrublands accounted for more than 85% of the area burned. Available agricultural census data indicates that all lands burned were under agricultural land use as of 1980 (sugarcane on Maui and pasture on O'ahu), but abandoned by the most recent census in 2015 (State of Hawai'i Office of Planning 2019; Perroy et al. 2016).

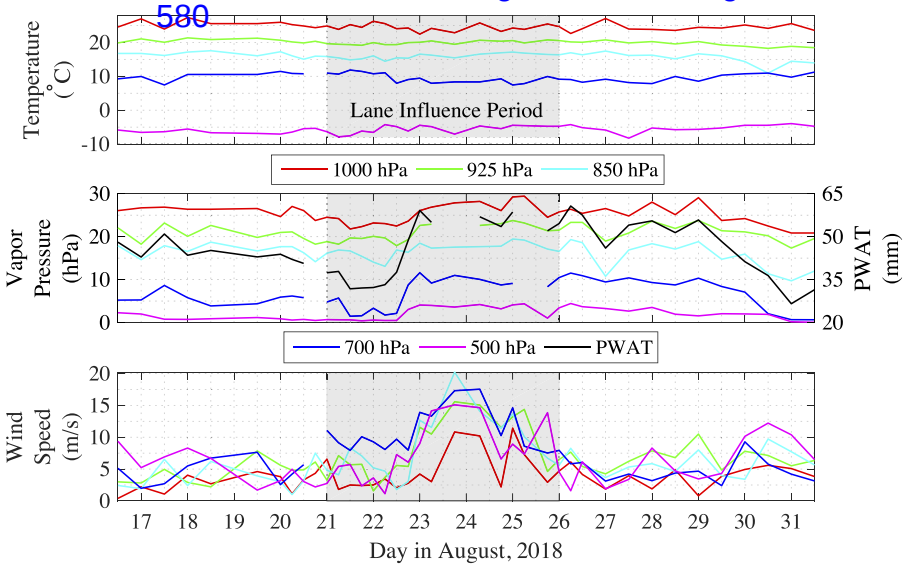

Fig. 4. Time series of (top) temperature (°C), (middle) vapor pressure (hPa), and (bottom) wind speed (m s^{-1}) from 16 to 31 Aug 2018 from the Hilo radiosonde balloon sounding (PHTO). The lowest five significant levels are included for each: 1000 (red), 925 (green), 850 (cyan), 700 (blue), and 500 hPa (magenta). PWAT (mm; black) is also included on the middle panel. The Lane influence period is shaded in light gray.

The causes of the Maui fire ignitions remain unknown; however, the Honolulu Fire Department attributed the O'ahu fire to arcing from electrical lines caused by high winds generated by Lane. Lightning was not a factor as there was little to no precipitation, and no thunderstorms near Maui or O'ahu at the time the fires began. The Kaua'ula and Kā'anapali fires on Maui required significant suppression resources including more than 70 county firefighters aided by state airport fire crews (Wilson 2018). Both fires grew rapidly within the first 12 h until approximately 1300 HST 25 August, after which the fires were contained and eventually extinguished approximately 30 h from the start time of the largest fire, the Kaua'ula Fire. On O'ahu, 54 firefighters worked to contain the blaze with strong, downsloping winds contributing to erratic fire behavior, grounding air support, and creating difficult conditions for suppression. According to land managers on site at the time of the fire, the downslope winds also appeared to help contain the fire within the bowl-shaped valley and prevent fire spread farther upslope into forested areas of the watershed (T. Anuheali'i 2018, personal communication).

Rainfall. While wildfires coincided with Lane on Maui and O'ahu, continuous long-duration rainfall plagued the island of Hawai'i. During the closest passage of Lane (22–25 August) the east (windward) side of the island of Hawai'i received nearly continuous rain. Over this 4-day period, the daily island areal means (calculated as the island means from the 250-m gridded surface) were 93, 121, 162, and 48 mm, respectively, and the 4-day event areal mean was 424 mm. A maximum single-day rainfall total (0000–0000 HST) of 646 mm (25 in.) was recorded at a meteorological station on the northeast side of the island of Hawai'i (at Pua'ākala) on 22 August and a 4-day event maximum of 1,444 mm (57 in.) was recorded to the southwest of Hilo at the Waiākea Uka station. Overall, the instrumental record (dating back to 1949) suggests that Lane was the wettest hurricane ever recorded in the state of Hawai'i (NWS 2018), and had the second highest storm total rainfall from a tropical cyclone in the United States, second only to Hurricane Harvey (2017) (Beven and Wroe 2019).

The spatial distribution of the rainfall during the Lane event on the island of Hawai'i is shown in Fig. 5. The highest precipitation totals were focused just to the west and southwest of Hilo on the eastern (windward) slopes of the island. The summits of the tallest mountains

(Mauna Kea and Mauna Loa) as well as the western (leeward) side remained fairly dry by comparison. Heavy rainfall also occurred on the exposed windward areas of Maui and O'ahu as the storm moved westward, however, it was not nearly as extreme as it was on the island of Hawai'i. The single station 4-day rainfall maxima over the same period, 22–25 August, for Maui and O'ahu, were 457 and 151 mm, respectively.

The 4-day Lane event produced more rainfall than any other 4-day period in the 25-year (1990–2014) gridded time series available for the island of Hawai'i. Areal mean rainfall for Lane (424 mm) was 43.2% greater than the largest 4-day total areal mean identified in the gridded time series (17–20 November 1990; 296 mm). The single-day station high during Lane (646 mm) was 22.3% greater than the largest daily rainfall recorded on the island of Hawai'i (528 mm) and 19.8% greater than the largest daily rainfall anywhere in the state (539 mm) within the 25-year daily rainfall record. The continuous and steady nature of the rainfall from Lane on the windward side of the island of Hawai'i over 4 days made this event especially notable.

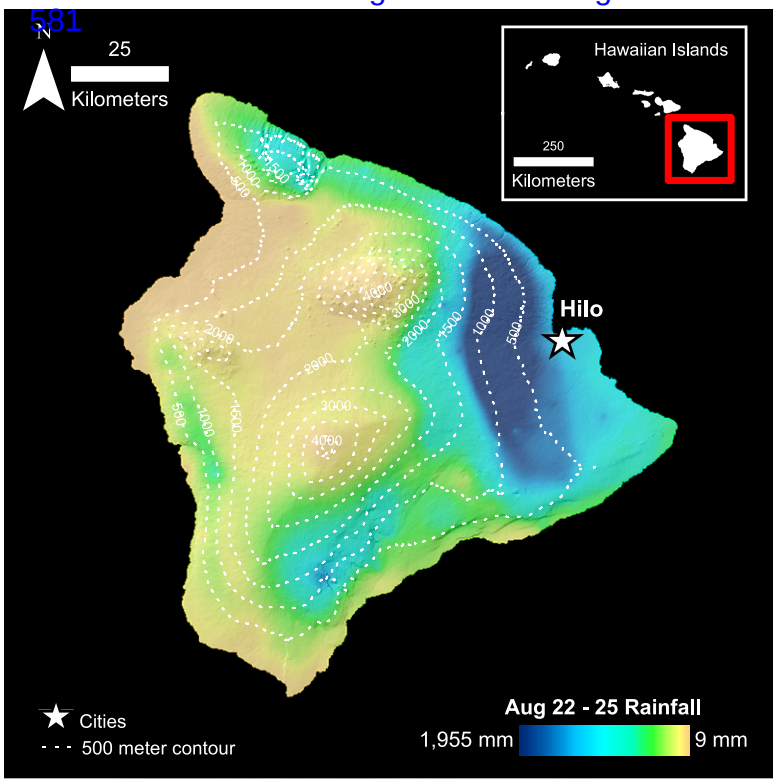

Fig. 5. Total accumulated rainfall (mm) during Hurricane Lane, from 22 to 25 Aug 2018 on the island of Hawai'i. Hillshade is included along with white dashed contours indicating terrain height every 500 m.

Impacts. The Hawaiian Islands suffered considerable damage as a result of the passage of Lane. Multiple wildfires in west Maui destroyed 21 structures and 30 vehicles, forced the evacuation of 100 homes, and the relocation of a hurricane shelter. Record-breaking rainfall caused severe flooding and landslides, leading to road closures across the island of Hawai'i. Road closures dramatically reduced accessibility, since impacted roads were often the *only* access roads, cutting off entire sections of coastline and communities from municipal resources and aid (see sidebar "Complications to emergency response"). For example, on 24 August, the only road along the windward (northeast) coast of the island of Hawai'i (Highway 19) was closed due to 14 landslides within a 25-mile stretch. Torrential rains also forced more than 100 people to evacuate from their homes on the island of Hawai'i, primarily in the area near Hilo. Poststorm assessments found 30 businesses and 152 homes damaged, 29 of the homes with major damage from flooding (Burnett 2018). On Maui, rainfall from Lane was blamed for one death, landslides there also blocked roadways, and one roadway collapsed due to a sinkhole (Peterkin 2018). The total estimate of damage costs for the state of Hawai'i (including damage from flood and fires) was US$250 million (Aon 2019).

Discussion

The simultaneous occurrence of extreme precipitation and wildfires during the passage of Lane provides a new perspective on the range of hazards associated with a hurricane event. Here, interactions between the atmospheric and biophysical conditions are discussed with respect to the hurricane environment to show how they exacerbated hazards and created favorable conditions for wildfires.

Fires on both Maui and O‘ahu ignited in areas dominated by nonnative grasses, known to respond quickly to changes in precipitation and contribute to fire risk both by accumulating biomass during wet periods and rapidly drying out during dry periods (Trauernicht 2019). The 2017/18 wet season (November–April) was relatively wet compared to historical means at most stations across the state (NWS/HFO 2018b) resulting in grass accumulation (Trauernicht 2019). During the 3 months leading up to Lane (May–July), a drying pattern was observed in leeward areas across the state with many leeward stations receiving <50% of their long-term average rainfall (NWS/HFO 2018b). In west Maui, the NOAA/NWS station located 140 m from the Lahaina fire reported rainfall 3% and 8% of the long-term average for the months of June and July, respectively, and over the 3 weeks leading up to the Lane event, only 5 mm of accumulated rainfall was observed at this location (NWS/HADS 2018). Dry conditions were also observed at a climate station ~4 km upslope of the O‘ahu fire. This pattern of wet months followed by dry months led to a surplus of dead, dry grass (i.e., fuel) on the ground, increasing the risk of fire.

Complications to Emergency Response

An additional hazard brought on by Lane arose from the limitations imposed on emergency managers. The simultaneous occurrences of high winds, fires, flooding, and landslides across the islands strained the capacity of emergency responders, limiting their ability to assist in other hurricane-related incidents, such as evacuations, medical emergencies, and road clearing. In some areas on the island of Hawai‘i, flooding and landslides led to road closures that essentially cut off entire sections of coastline and communities from municipal resources and aid.

The majority of the state’s 1.43 million people and associated infrastructure are located in coastal zones and thus highly vulnerable to the many hazards associated with the passage of a hurricane. Current storm emergency response plans involve sheltering in place or moving inland to areas of higher elevation (Wolshon et al. 2005). Furthermore, the state is more than 3,900 km from the continental United States, complicating and delaying the arrival of outside emergency assistance in the wake of a natural disaster. A recent analysis by the Hawai‘i Emergency Management Agency highlighted the vulnerability associated with having only one harbor capable of accommodating high-volume container ships and only a 5–7-day supply of food available in the islands at any given time (Hara 2018). The population of the state is expected to reach 1.65 million by 2045 (Kim et al. 2018), which will put additional strains on food supplies, land resources, and emergency response.

To fully understand the vulnerability of populations to extreme weather events such as Lane, the full spectrum of risk associated with the natural hazards produced by an event and the social responses to these hazards must be considered. For Hawai‘i, this is especially important considering access to emergency services from the U.S. mainland is limited and, in the event that damage occurs to the shipping ports or airports, access to the islands and the distribution of emergency supplies could be compromised.

Over the days of Lane’s approach and preceding wildfire ignitions, drought conditions steadily worsened as indicated by the KBDI. Under well-developed drought, the condition of the vegetation (e.g., plant moisture content and the proportion of dead to live vegetation) was well suited to support combustion. Compounding these drought conditions on the ground, the atmospheric conditions as Lane approached exacerbated the risk of fire. Wind is the primary driver of fire spread, which can develop especially rapidly in the fine, grassy fuels that dominated the burn areas (Cheney and Sullivan 2008). It can also contribute to ignitions by knocking down power lines, as observed with the O‘ahu fire. The recorded strong, erratic winds at both locations grounded helicopters, which are a critical resource for fire suppression in Hawai‘i’s steep terrain.

The geographical location of the fires on exposed leeward slopes, the reports from local fire officials, and the observed strong winds on both Maui and O‘ahu suggest that dynamically driven downslope winds (Elvidge and Renfrew 2016) contributed to the occurrence and spread of fire during Lane. Downslope winds on the lee sides of the Hawaiian Islands are common, and enhanced wind speeds from the hurricane environment at the 850- and 700-hPa levels (Fig. 4) likely amplified these winds further. Downslope winds occur once orographically lifted air transits the peak of a mountain and begins to descend on the lee side, resulting in an increase in speed, and often both warming and drying of the air due to its descent, and

due to mixing of upper-level dry air downward. This typical signature of warm, dry air in the downslope wind is not visible during Lane from the surface stations, but relatively dry air was present in the midlevels (Fig. 4).

A distinct drying signal was seen as Lane approached the state. Weak broadscale subsidence is often found just outside the periphery of a hurricane, characterized by slowly sinking air that is warm and dry, as a result of compression upon descent. Prior work showed this subsidence region surrounding a storm visible from satellite images as a cloud-free ring (Fett 1964). Water vapor channel satellite images (not shown) of Lane as it approached the state (19–21 August) clearly showed a similar dry, cloud-free ring or "hurricane lei" (a term coined here) surrounding Lane, which is a result of either subsidence or advection of dry air around the storm periphery. The hurricane lei effect can be seen in the surface stations as a drop in the minimum RH, precipitable water (PWAT), and vapor pressure prior to Lane's arrival on 21–22 August (Figs. 3 and 4). Although lower RH increases fire intensity and rate of spread, the observed atmospheric drying in the hurricane lei occurred prior to the fire ignitions and therefore did not directly contribute to fire danger in this case. Instead, longer term drought conditions strongly contributed to fire potential due to its effect on fuel curing, and the elevated wind speeds in the storm environment were the largest direct factor influencing fire development. Low humidity in the atmosphere increases fire risk over short-term (hourly) time scales by decreasing fuel moisture in standing vegetation, thereby increasing the likelihood of combustion and the energy released by the fire (i.e., fire intensity, Viney 1991; Beverly and Wotton 2007). While low humidity was not a factor during the Lane event, the potential for the hurricane lei drying effect to enhance fire risk should not be overlooked. Three weeks prior to Lane, the approach of Hurricane Hector was also associated with low humidity, and large fires on O'ahu and the island of Hawai'i raised concerns among NWS forecasters over increased fire intensity due to the abnormally dry conditions (D. Wroe 2018, personal communication). Moreover, Hawai'i has some of the highest recorded densities of wildfire ignitions (e.g., number of fires per square kilometer per year), caused primarily by human activity (Trauernicht and Lucas 2016) and, thus, has near-constant risk of wildfire initiation.

Extreme rainfall due to the interaction of tropical cyclones with mountains is common (DeHart and Houze 2017; Smith et al. 2009; Li et al. 2007; Wu et al. 2002). Many important criteria for heavy orographic precipitation were present during Lane including a moisture rich environment, steady upslope winds, and the presence of a large, preexisting, slow-moving, convective system (Lin et al. 2001). The moisture rich environment is visible as an increase in PWAT (22 August) that coincides with an increase in the 700-hPa vapor pressure, suggesting a deepening of the marine boundary layer (Fig. 4). The deepening is accompanied by a slight simultaneous downward shift in the 700-hPa temperature consistent with the disappearance of the trade wind inversion. Without this low-level temperature inversion, deep convection can more easily develop in the environment. Finally, enhanced winds at mid- and upper levels concurrent with these moist unstable conditions led to strong wind shear between 850 and 500 hPa, which intensified convection and helped to bring extreme rainfall to the island of Hawai'i (Callaghan 2019).

The presence of these important ingredients for extreme rainfall makes it no surprise that Lane produced a record-breaking rainfall event. The simultaneous occurrence of extreme precipitation and wildfires, however, is uncommon and provides a new perspective on the range of hazards associated with a hurricane event under certain biophysical and atmospheric conditions. The fires on Maui and O'ahu are explained by a number of these interacting conditions. First, all of the fires occurred in areas dominated by nonnative grasses. Second, the wet and then dry rainfall pattern preceding the event created an abundance of fuel. Finally, windy conditions were driven by the storm environment and topography. Consequently, the fires spread rapidly across the landscape due to the abundance of fine, grassy fuels and strong

winds creating firefighting conditions the deputy fire chief described as "some of the most adverse the Maui Fire Department has faced in recent history" (Osher 2018).

While the Lane example is only one case study connecting a hurricane to fires, future changes are expected to increase the risk of both in Hawai'i. Over the last 60 years, Hawai'i has seen >60% decline statewide in the land areas under agricultural production, including cultivated crops and ranching (Trauernicht et al. 2015; Perroy et al. 2016). These abandoned agricultural lands are now covered with the same nonnative fire-prone grasses and shrubs that burned during Lane, which currently comprise nearly 25% of state land. With rising costs of labor and the increasing value of real estate in Hawai'i, continued declines in agricultural production are replaced by increased residential development (Suryanata 2002). These land-use changes are compounded by an observed trend of drying in the area (Frazier and Giambelluca 2017), both of which are expected to further increase the risk of fire in Hawai'i in the future (Trauernicht 2019). As for the connection of fire and hurricanes, we note that hurricane season in the central Pacific (1 June–30 November) coincides with the dry season (May–October) and the climatological peak in KBDI, illustrating an ongoing connection between hurricanes and fire risk in Hawai'i that requires further investigation.

Hurricane risk in Hawai'i and the Pacific region in general is also expected to increase. A warming climate increases the amount of energy available to fuel storms, thus supporting the formation of stronger storms (Knutson et al. 2010; Bengtsson et al. 2007; Bender et al. 2010) and an increase in storm driven precipitation (e.g., Knutson et al. 2010; O'Gorman and Schneider 2009). Another influence on precipitation comes from a projected global slow-down of storm translation speed (Kossin 2018) allowing local precipitation totals to increase when a storm spends more time over a given location. Finally, studies suggest a poleward shift of the location of storm maximum intensity (Kossin et al. 2014). For Hawai'i specifically, changes in the North Pacific semipermanent high pressure ridge and changes in the strength of vertical wind shear in a changing climate are important. Projections by Murakami et al. (2012) showed an increase in tropical cyclones in the central Pacific near Hawai'i by late century.

Concluding remarks

Lane brought to light the risk of compounding hazards associated with the passage of a hurricane in the Hawaiian region. From this study we document what we believe to be the first instance of a hurricane causing both heavy rainfall and contributing to multiple instances of fire simultaneously. Future research efforts are needed to examine whether this is an isolated instance, or whether these types of compounding hazards have occurred elsewhere or previously. Additional research will help to determine if this particular instance of hurricane–fire connection is an artifact of global changes to the global climate system that may become more common in the future. A complete understating of these factors is critical to understanding the vulnerability of people and resources exposed during a severe weather event. This is especially of interest in the context of a changing climate where intensity and frequency of compounding extreme events is likely to increase (e.g., Mora et al. 2018).

Acknowledgments. We appreciate constructive criticism from three reviewers, and discussions with the National Weather Service (NWS) Honolulu Forecast Office (HFO), especially Kevin Kodama, who provided additional rainfall datasets and knowledge of the storm precipitation and hydrology. *GOES-5* images were provided by Randall Alliss (Northrop Grumman Corporation), and support for the Hawai'i EPSCoR Program is provided by the National Science Foundation's Research Infrastructure Improvement (RII) Track-1: 'Ike Wai: Securing Hawai'i's Water Future' Award OIA-1557349.

References

Aon, 2019: Weather, climate & catastrophe insight: 2018 annual report. Aon plc, 86 pp., http://thoughtleadership.aonbenfield.com/Documents/20190122-ab-if-annual-weather-climate-report-2018.pdf.

Barbero, R., J. T. Abatzoglou, C. A. Kolden, K. C. Hegewisch, N. K. Larkin, and H. Podschwit, 2015: Multi-scalar influence of weather and climate on very large-fires in the eastern United States. *Int. J. Climatol.*, **35**, 2180–2186, https://doi.org/10.1002/joc.4090.

Bender, M. A., T. R. Knutson, R. E. Tuleya, J. J. Sirutis, G. A. Vecchi, S. T. Garner, and I. M. Held, 2010: Modeled impact of anthropogenic warming on the frequency of intense Atlantic Hurricanes. *Science*, **327**, 454–458, https://doi.org/10.1126/science.1180568.

Bengtsson, L., K. I. Hodges, M. Esch, N. Keenlyside, L. Kornblueh, J.-J. Luo, and T. Yamagata, 2007: How may tropical cyclones change in a warmer climate? *Tellus*, **59A**, 539–561, https://doi.org/10.1111/j.1600-0870.2007.00251.x.

Beven, J. L., II, and D. Wroe, 2019: Hurricane Lane (EP142018), 15-28 August 2018. NHC Tropical Cyclone Rep., 28 pp., www.nhc.noaa.gov/data/tcr/EP142018_Lane.pdf.

Beverly, J., and M. Wotton, 2007: Modelling the probability of sustained flaming: Predictive value of fire weather index components compared with observations of site weather and fuel moisture conditions. *Int. J. Wildland Fire*, **16**, 161, https://doi.org/10.1071/WF06072.

Brolley, J., J. O'Brien, J. Schoof, and D. Zierden, 2007: Experimental drought threat forecast for Florida. *Agric. For. Meteor.*, **145**, 84–96, https://doi.org/10.1016/j.agrformet.2007.04.003.

Brown, R. H., D. Josephson, J. Elbert, and W. Friday, 1993: Hurricane Iniki, September 6-13, 1992. National Disaster Survey Rep., NOAA, 111 pp., www.weather.gov/media/publications/assessments/iniki1.pdf.

Burnett, J., 2018: Damage to county infrastructure caused by Lane totals about $20M. *Hawaii Tribune-Herald*, 14 September, www.hawaiitribune-herald.com/2018/09/14/hawaii-news/damage-to-county-infrastructure-caused-by-lane-totals-about-20m/.

Businger, S., M. P. Nogelmeier, P. W. U. Chinn, and T. Schroeder, 2018: Hurricane with a history: Hawaiian newspapers illuminate an 1871 storm. *Bull. Amer. Meteor. Soc.*, **99**, 137–147, https://doi.org/10.1175/BAMS-D-16-0333.1.

Callaghan, J., 2019: A short note on the intensification and extreme rainfall associated with Hurricane Lane. *Trop. Cyclone Res. Rev.*, **8**, 103–107, https://doi.org/10.1016/j.tcrr.2019.07.010.

Cheney, P., and A. Sullivan, 2008: *Grassfires: Fuel, Weather and Fire Behaviour.* 2nd ed. CSIRO Publishing, 160 pp.

Christopher, S. A., P. Gupta, U. Nair, T. A. Jones, S. Kondragunta, Y. Wu, J. Hand, and X. Zhang, 2009: Satellite remote sensing and mesoscale modeling of the 2007 Georgia/Florida fires. *IEEE J. Sel. Top. Appl. Earth Obs. Remote Sens.*, **2**, 163–175, https://doi.org/10.1109/JSTARS.2009.2026626.

Coral Reef Watch, 2019: NOAA Coral Reef Watch Version 3.0 Daily Global 5-km Satellite Virtual Station Time Series Data for the Hawaiian Islands, Aug. 1, 2018 - Aug. 31, 2018. National Ocean and Atmospheric Administration, accessed 7 March 2019, https://coralreefwatch.noaa.gov/vs/data.php.

Corbosiero, K. L., and J. Molinari, 2003: The relationship between storm motion, vertical wind shear, and convective asymmetries in tropical cyclones. *J. Atmos. Sci.*, **60**, 366–376, https://doi.org/10.1175/1520-0469(2003)060<0366:TRBSMV>2.0.CO;2.

DeHart, J. C., and R. A. Houze, 2017: Orographic modification of precipitation processes in Hurricane Karl (2010). *Mon. Wea. Rev.*, **145**, 4171–4186, https://doi.org/10.1175/MWR-D-17-0014.1.

Dolling, K., P.-S. Chu, and F. Fujioka, 2005: A climatological study of the Keetch/Byram drought index and fire activity in the Hawaiian Islands. *Agric. For. Meteor.*, **133**, 17–27, https://doi.org/10.1016/j.agrformet.2005.07.016.

Drusch, M., and Coauthors, 2012: Sentinel-2: ESA's optical high-resolution mission for GMES operational services. *Remote Sens. Environ.*, **120**, 25–36, https://doi.org/10.1016/j.rse.2011.11.026.

Elvidge, A. D., and I. A. Renfrew, 2016: The causes of foehn warming in the lee of mountains. *Bull. Amer. Meteor. Soc.*, **97**, 455–466, https://doi.org/10.1175/BAMS-D-14-00194.1.

FDEM, 2011: Appendix G: State of Florida wildfire hazard mitigation plan annex. Tech. rep., Florida Division of Emergency Management, 219 pp., www.floridadisaster.org/contentassets/c6a7ead876b1439caad3b38f7122d334/appendix-g_wildfire-hazard-mitigation-plan-annex.pdf.

FEMA, 2018: President Donald J. Trump approves major disaster declaration for Hawaii. U.S. Department of Homeland Security, Federal Emergency Management Agency, www.fema.gov/news-release/2018/09/28/president-donald-j-trump-approves-major-disaster-declaration-hawaii.

Fernandes, P., 2018: Avoiding disastrous wildfires in Europe. *Science eLetters, https://science.sciencemag.org/content/359/6379/1001.2/tab-e-letters.*

Fett, R. W., 1964: Aspects of hurricane structure: New model considerations suggested by TIROS and Project Mercury observations. *Mon. Wea. Rev.*, **92**, 43–60, https://doi.org/10.1175/1520-0493(1964)092<0043:AOHSNM>2.3.CO;2.

Frazier, A. G., and T. W. Giambelluca, 2017: Spatial trend analysis of Hawaiian rainfall from 1920 to 2012. *Int. J. Climatol.*, **37**, 2522–2531, https://doi.org/10.1002/joc.4862.

Giambelluca, T. W., Q. Chen, A. G. Frazier, J. P. Price, Y.-L. Chen, P.-S. Chu, J. K. Eischeid, and D. M. Delparte, 2013: Online rainfall atlas of Hawai'i. *Bull. Amer. Meteor. Soc.*, **94**, 313–316, https://doi.org/10.1175/BAMS-D-11-00228.1.

Hara, K. S., 2018: All-hazards preparedness improvement action plan and report. State of Hawai'i, Department of Defense, 36 pp., https://dod.hawaii.gov/hiema/files/2018/02/Preparedness-Report-18FEB2018.pdf.

Kim, Y.-S., J. Bai, and E. Tian, 2018: Population and economic projections for the state of Hawaii to 2045. Research and Economic Analysis Division Department of Business, Economic Development and Tourism, State of Hawaii, 34 pp., http://files.hawaii.gov/dbedt/economic/data_reports/2045-long-range-forecast/2045-long-range-forecast.pdf.

Klemas, V., J. Dobson, R. L. Ferguson, and K. D. Haddad, 1993: A coastal land cover classification system for the NOAA coastwatch change analysis project. *J. Coastal Res.*, **9**, 862–872.

Klotzbach, P., and M. Bell, 2018: Northeast Pacific Ocean historical tropical cyclone statistics. Colorado State University, http://tropical.atmos.colostate.edu/Realtime/index.php?arch&loc=global.

Knapp, K. R., M. C. Kruk, D. H. Levinson, H. J. Diamond, and C. J. Neumann, 2010: The International Best Track Archive for Climate Stewardship (IBTrACS): Unifying tropical cyclone data. *Bull. Amer. Meteor. Soc.*, **91**, 363–376, https://doi.org/10.1175/2009BAMS2755.1.

Knutson, T. R., and Coauthors, 2010: Tropical cyclones and climate change. *Nat. Geosci.*, **3**, 157–163, https://doi.org/10.1038/ngeo779.

Kossin, J. P., 2018: A global slowdown of tropical-cyclone translation speed. *Nature*, **558**, 104–107, https://doi.org/10.1038/s41586-018-0158-3.

——, K. A. Emanuel, and G. A. Vecchi, 2014: The poleward migration of the location of tropical cyclone maximum intensity. *Nature*, **509**, 349–352, https://doi.org/10.1038/nature13278.

Li, Y., W. Huang, and J. Zhao, 2007: Roles of mesoscale terrain and latent heat release in typhoon precipitation: A numerical case study. *Adv. Atmos. Sci.*, **24**, 35–43, https://doi.org/10.1007/s00376-007-0035-8.

Lin, Y.-L., S. Chiao, T.-A. Wang, M. L. Kaplan, and R. P. Weglarz, 2001: Some common ingredients for heavy orographic rainfall. *Wea. Forecasting*, **16**, 633–660, https://doi.org/10.1175/1520-0434(2001)016<0633:SCIFHO>2.0.CO;2.

Liu, K., H. Lu, and C. Shen, 2008: A 1200-year proxy record of hurricanes and fires from the Gulf of Mexico coast: Testing the hypothesis of hurricane-fire interactions. *Quat. Res.*, **69**, 29–41, https://doi.org/10.1016/j.yqres.2007.10.011.

Lonfat, M., F. D. Marks, and S. S. Chen, 2004: Precipitation distribution in tropical cyclones using the Tropical Rainfall Measuring Mission (TRMM) Microwave Imager: A global perspective. *Mon. Wea. Rev.*, **132**, 1645–1660, https://doi.org/10.1175/1520-0493(2004)132<1645:PDITCU>2.0.CO;2.

Longman, R. J., and Coauthors, 2018: Compilation of climate data from heterogeneous networks across the Hawaiian Islands. *Sci. Data*, **5**, 180012, https://doi.org/10.1038/sdata.2018.12.

——, and Coauthors, 2019: High-resolution gridded daily rainfall and temperature for the Hawaiian islands (1990–2014). *J. Hydrometeor.*, **20**, 489–508, https://doi.org/10.1175/JHM-D-18-0112.1.

Mora, C., and Coauthors, 2018: Broad threat to humanity from cumulative climate hazards intensified by greenhouse gas emissions. *Nat. Climate Change*, **8**, 1062–1071, https://doi.org/10.1038/s41558-018-0315-6.

Murakami, H., R. Mizuta, and E. Shindo, 2012: Future changes in tropical cyclone activity projected by multi-physics and multi-SST ensemble experiments using the 60-km-mesh MRI-AGCM. *Climate Dyn.*, **39**, 2569–2584, https://doi.org/10.1007/s00382-011-1223-x.

Myers, R. K., and D. H. van Lear, 1998: Hurricane-fire interactions in coastal forests of the south: A review and hypothesis. *For. Ecol. Manage.*, **103**, 265–276, https://doi.org/10.1016/S0378-1127(97)00223-5.

NOAA/CPHC, 2018: Hurricane Walaka Intermediate Advisory Number 18a. NOAA/Pacific Regional Headquarters Central Pacific Hurricane Center, www.nhc.noaa.gov/archive/2018/cp01/cp012018.public_a.018.shtml?.

——, 2019: CPHC Tropical Cyclone Product Archives. NOAA/Central Pacific Hurricane Center, www.nhc.noaa.gov/data/.

NOAA/NCEI, 2018: State of the Climate: Global Climate Report for September 2018. NOAA/National Centers for Environmental Information, www.ncdc.noaa.gov/sotc/global/201809.

——, 2019: State of the Climate: Global Climate Report for Annual 2018. NOAA/National Centers for Environmental Information, www.ncdc.noaa.gov/sotc/global/201813.

NOAA/NHC, 2019: 2018 Tropical Cyclone Advisory Archive. National Hurricane Center, www.nhc.noaa.gov/archive/2018/.

NWS, 2018: Public information statement, 459 AM HST Sun Aug 26 2018. National Weather Service Public Weather Statement, http://mesonet.agron.iastate.edu/wx/afos/p.php?pil=PNSHFO&e=201808261459.

NWS/HADS, 2018: Hydrometeorological Automated Data System. NOAA/National Weather Service, https://hads.ncep.noaa.gov/.

NWS/HFO, 2018a: Fire Weather Operations Plan. NOAA/National Weather Service, Honolulu Forecast Office, www.prh.noaa.gov/hnl/pages/Firewxops.doc.

——, 2018b: Monthly precipitation summary for the state of Hawaii. NOAA/NWS, www.weather.gov/hfo/hydro_summary.

O'Gorman, P. A., and T. Schneider, 2009: The physical basis for increases in precipitation extremes in simulations of 21st-century climate change. *Proc. Natl. Acad. Sci. USA*, **106**, 14773–14777, https://doi.org/10.1073/pnas.0907610106.

Osher, W., 2018: Conditions "unprecedented" in battling west Maui fires during hurricane warning. *Maui Now*, 27 August, https://mauinow.com/2018/08/27/conditions-unprecedented-in-battling-west-maui-fires-during-hurricane-warning/.

Perroy, R. L., J. Melrose, and S. Cares, 2016: The evolving agricultural landscape of post-plantation Hawai'i. *Appl. Geogr.*, **76**, 154–162, https://doi.org/10.1016/j.apgeog.2016.09.018.

Peterkin, O., 2018: Heavy rains, flooding brought by Lane deals serious damage to Maui roads. *Hawaii News Now*, 26 August, www.hawaiinewsnow.com/story/38962760/heavy-rains-flooding-brought-by-lane-deals-serious-damage-to-maui-roads/.

Platt, W. J., B. Beckage, R. F. Doren, and H. H. Slater, 2002: Interactions of large-scale disturbances: Prior fire regimes and hurricane mortality of savanna pines. *Ecology*, **83**, 1566–1572, https://doi.org/10.1890/0012-9658(2002)083[1566:IOLSDP]2.0.CO;2.

Rappaport, E. N., 2014: Fatalities in the United States from atlantic tropical cyclones: New data and interpretation. *Bull. Amer. Meteor. Soc.*, **95**, 341–346, https://doi.org/10.1175/BAMS-D-12-00074.1.

Smith, J. M., A. B. Kennedy, J. J. Westerink, A. A. Taflanidis, and K. F. Cheung, 2012: Hawaii hurricane wave and surge modeling and fast forecasting. *Coastal Eng. Proc.*, **1**, 8, https://doi.org/10.9753/icce.v33.management.8.

Smith, R. B., P. Schafer, D. Kirshbaum, and E. Regina, 2009: Orographic enhancement of precipitation inside Hurricane Dean. *J. Hydrometeor.*, **10**, 820–831, https://doi.org/10.1175/2008JHM1057.1.

State of Hawaii Office of Planning, 2019: Hawaii Statewide GIS Program. State of Hawaii, http://planning.hawaii.gov/gis/.

Suryanata, K., 2002: Diversified agriculture, land use, and agrofood networks in Hawaii. *Econ. Geogr.*, **78**, 71, https://doi.org/10.2307/4140824.

Svoboda, M., and Coauthors, 2002: The Drought Monitor. *Bull. Amer. Meteor. Soc.*, **83**, 1181–1190, https://doi.org/10.1175/1520-0477-83.8.1181.

Trauernicht, C., 2019: Vegetation-rainfall interactions reveal how climate variability and climate change alter spatial patterns of wildland fire probability on Big Island, Hawaii. *Sci. Total Environ.*, **650**, 459–469, https://doi.org/10.1016/j.scitotenv.2018.08.347.

——, and M. P. Lucas, 2016: Wildfire ignition density maps for Hawaii. Forest and Natural Resource Management Series RM-21, University of Hawai'i Cooperative Extension Service, www.ctahr.hawaii.edu/oc/freepubs/pdf/RM-21.pdf.

——, E. Pickett, C. P. Giardina, C. M. Litton, S. Cordell, and A. Beavers, 2015: The contemporary scale and context of wildfire in Hawai'i. *Pac. Sci.*, **69**, 427–444, https://doi.org/10.2984/69.4.1.

Turner, R. K., S. Subak, and W. N. Adger, 1996: Pressures, trends, and impacts in coastal zones: Interactions between socioeconomic and natural systems. *Environ. Manage.*, **20**, 159–173, https://doi.org/10.1007/BF01204001.

Viney, N., 1991: A review of fine fuel moisture modelling. *Int. J. Wildland Fire*, **1**, 215, https://doi.org/10.1071/WF9910215.

Willmott, C. J., and S. M. Robeson, 1995: Climatologically aided interpolation (CAI) of terrestrial air temperature. *Int. J. Climatol.*, **15**, 221–229, https://doi.org/10.1002/joc.3370150207.

Wilson, C., 2018: Wind-whipped fire ravages Lahaina hillsides, destroys 21 structures. *Honolulu Star Advertiser*, 26 August, www.staradvertiser.com/2018/08/26/hawaii-news/wind-whipped-fire-ravages-lahaina-hillsides-destroys-21-structures/.

Wolshon, B., E. Urbina Hamilton, M. Levitan, and C. Wilmot, 2005: Review of policies and practices for hurricane evacuation. II: Traffic operations, management, and control. *Nat. Hazards Rev.*, **6**, 143–161, https://doi.org/10.1061/(ASCE)1527-6988(2005)6:3(143).

Wu, C.-C., T.-H. Yen, Y.-H. Kuo, and W. Wang, 2002: Rainfall simulation associated with typhoon Herb (1996) near Taiwan. Part I: The topographic effect. *Wea. Forecasting*, **17**, 1001–1015, https://doi.org/10.1175/1520-0434(2003)017<1001:RSAWTH>2.0.CO;2.